# Theoretical Study of the $CO_2$ Adsorption by Zeolitic Imidazolate Frameworks (ZIFs)



| | |
|---|---|
| Journal: | *The Journal of Physical Chemistry* |
| Manuscript ID | jp-2017-04977t.R2 |
| Manuscript Type: | Article |
| Date Submitted by the Author: | 26-Aug-2017 |
| Complete List of Authors: | Izzaouihda, Safia; Facu, CHIMIE<br>Abou El Makarim, Hassna; University Mohammed V, Faculty of Sciences<br>Benoit, David; University of Hull, Chemistry<br>Komiha, Najia; University Mohammed V, Faculty of Sciences |
| | |

# Theoretical Study of the $CO_2$ Adsorption by Zeolitic Imidazolate Frameworks (ZIFs)

**Safia IZZAOUIHDA[1*], Hassna ABOU El MAKARIM[1], David M. BENOIT[2], Najia KOMIHA[1*]**

[1]Laboratory LS3ME, Team Theoretical Chemistry and Molecular Modeling, University of Mohammed V Faculty of Sciences, Department of Chemistry, BP1014 Rabat Morocco
[2]E.A. Milne Centre for Astrophysics & G.W. Gray Centre for Advanced Materials, Chemistry, School of Mathematical and Physical Sciences, University of Hull, Hull, HU6 7RX, UK

*Corresponding authors: komiha@fsr.ac.ma; safiafssm@gmail.com

## Abstract

Density functional theory with Grimme's empirical correction, DFT-D3, has been used to examine the adsorption of a carbon dioxide molecule by different sets of zeolitic imidazolate framework materials (ZIF-1 to -4, -6 to -10, and -zni). We have calculated the interaction energy, the dipole moment variation, and the charge density difference for the different $CO_2$@ZIF structures. Our study shows a strong relationship between the $CO_2$ adsorption energy and the volume of the cavities of the ZIFs: the capture of carbon dioxide depends on the shape and size of the ZIFs pore in which $CO_2$ has been inserted. The physisorption phenomena that govern the adsorption of $CO_2$ molecule require both π-stacking interactions and hydrogen-like bonding. We have found that adsorption does not change the geometry of $CO_2$, but it induces a significant structural change in some ZIF structures.

## 1. Introduction

The increasing concentration of $CO_2$ gas in the atmosphere is one of the major concerns of the scientific community today. Numerous studies have begun to explore this topic and propose solutions to reduce the high concentration of this greenhouse gas.

Using copolymerization of either Zn(II) or Co(II) ions with imidazolate-type linkers (Im), Yaghi and his co-workers have pioneered the synthesis of new materials which possess both a high porosity and an excellent chemical stability: the zeolitic imidazolate frameworks (ZIFs) [1]. These new classes of porous crystals are named so due to their structural proximity to zeolites. The equilibrium value of the angle M-Im-M in ZIFs (where M stands for Zn or Co cations and Im stands for the imidazolate linker) is 145 ° which is equal to the Si-O-Si angle in zeolites [2]. The development and recent progress of different synthesis strategies to generate ZIF materials have been analyzed and summarized by Chen et al [3].

Zeolitic imidazolate frameworks have an exceptional ability to capture and separate $CO_2$ from a gas mixture. A series of ZIFs have been recently examined for their potential to separate $CO_2$ from $CH_4$, CO, $O_2$ and $N_2$ gases [4,5]. The nature of the interaction between $CO_2$ and ZIFs has been the subject of numerous theoretical studies [6–9]. Understanding the physical phenomena governing this interaction is of academic as well as industrial importance. Different studies have approached this issue by investigating the interaction of $CO_2$ with ZIF organic units. The interactions between imidazole and $CO_2$ molecules are mainly dominated by Van der Waals forces, including induction, dispersion and electrostatic effects [10]. Moreover, the proposed $CO_2$@[$Zn^{q+}$Im] (where q = 0,1, 2; Im = imidazole) models of the interactions of $CO_2$ with these subunits of zeolitic imidazolate frameworks show that $CO_2$ molecules can be adsorbed through π-stacking as well as σ-type hydrogen-bonding interactions [11]. The aim of the present work is to study the physisorption properties of $CO_2$ with a set of ZIF materials. We have limited this work to compounds with chemical composition $Zn(Im)_2$.

This paper is structured as follows: Section 2 describes the details of the computational approach used to generate our results. In section 3, we present the optimized set of ZIFs structures (section 3.1) which are used as a starting point to trapping a single $CO_2$ molecule. In section 3.2 we report our DFT and DFT-D3 calculations for adsorbed $CO_2$ molecules in the cavities of the ZIF. The analysis of the charge density transformation in $CO_2$@ZIFs complexes are reported in subsection 3.3. The last section is reserved to our conclusions.

## 2. Computational methods

In this study, we have adopted periodical calculations using the QUICKSTEP module [12] built in the CP2K program [13] which allows DFT calculations [14,15]. This module uses the GPW method [16] allowing a better treatment of the electrostatic interactions. The GGA functional PBE [17] has been used to describe exchange-correlation effects.

We consider ZIF structures that have been synthesized as crystals by copolymerization of Zn(II) with imidazolate-type linkers by Yaghi and his co-workers [1]: ZIF-1, -2, -3, -4, -6 and 10, and the one (zni) synthesized by Lehnert and Seel [18]. Moreover, we also investigate the theoretical imidazolate $Zn(Im)_2$ models, ZIF-7, ZIF-8 and ZIF-9 obtained by Lewis et al. [19] by the removal of substituents from the imidazolate rings (-CH3, $-C_6H_4$). The ZIF details have been extracted from the crystallographic data base CCDC [20], eliminating extra-framework species and the imidazolate substituents when required.

To improve the description of the long-range dispersion interactions, we have used the DFT-D3 method where DFT is corrected using an empirical Van der Waals correction suggested by Grimme et al. [21]. For each atom we have used the TZV2P MOLOPT-GTH basis set [22] except for Zn atoms for which we have used a DZVP MOLOPT-GTH basis[22]. The GTH pseudopotentials in our calculations have been generated from fully relativistic all-electrons calculations for each atom[23–25].

Furthermore, to minimize the total ground state energy, we have used the orbital transformation method (OT) [26], where all calculations have been performed at the Γ–point of the Brillouin zone. Periodic boundary conditions have been applied in xyz directions. The BFGS optimization method has been used for all the calculations using default convergence criteria and default energy SCF convergence criterion of $10^{-5}$ Hartree.

# 3. Results and discussion

## 1. Geometry optimization of ZIF structures

In the first stage, we have performed a geometry optimization to determine the equilibrium structures for the different ZIFs (ZIF-1 to -4, -6 to 10, and zni). The total energy has been calculated using both DFT/PBE and PBE-D3 methods, the latter leading to an improvement of the long-range dispersion interactions. Table 1 summarizes the calculations results along with volume and framework density.

| ZIFs | Composition | CCDC Code | Number of Zn atoms per unit | Volume in Å$^3$ | Framework density (Zn/Volume) in nm$^{-3}$ | E $_{ZIFs}$ in eV/Zn | |
|---|---|---|---|---|---|---|---|
| | | | | | | DFT/PBE | DFT/PBE-D3 |
| 1 | $Zn(Im)_2$ | VEJYEP | 8 | 2310.2 [a] | 3.46 [a] | –3757.010 | –3757.660 |
| | | | | 2195.8 [b] | 3.64 [b] | | |
| 2 | $Zn(Im)_2$ | VEJYIT | 16 | 5691.6 [a] | 2.81 [a] | –3756.990 | –3757.561 |
| | | | | 5706.6 [b] | 2.80 [b] | | |
| 3 | $Zn(Im)_2$ | VEJYOZ | 16 | 6031.4 [a] | 2.65 [a] | –3757.009 | –3757.579 |
| | | | | 6024.1 [b] | 2.66 [b] | | |
| 4 | $Zn(Im)_2$ | VEJYUF | 16 | 4380.5 [a] | 3.65 [a] | –3757.014 | –3757.680 |
| | | | | 4344.9 [b] | 3.68 [b] | | |
| 6 | $Zn(Im)_2$ | EQOCOC | 8 | 3594.3 [a] | 2.22 [a] | –3757.019 | –3757.560 |
| | | | | 3470.0 [b] | 2.31 [b] | | |
| 7* | $Zn(Im)_2$ | – | 6 | 2427.1 [a] | 2.47 [a] | –3756.973 | –3757.530 |
| | | | | 2404.8 [b] | 2.50 [b] | | |
| 8* | $Zn(Im)_2$ | – | 6 | 2474.7 [a] | 2.42 [a] | –3757.021 | –3757.589 |
| | | | | 2452.6 [b] | 2.47 [b] | | |
| 9* | $Zn(Im)_2$ | – | 18 | 7223.9 [a] | 2.49 [a] | –3756.973 | –3757.533 |
| | | | | 7178.9 [b] | 2.51 [b] | | |
| 10 | $Zn(Im)_2$ | VEJZIU | 16 | 7312.7 [a] | 2.19 [a] | –3757.024 | –3757.572 |
| | | | | 7105.4 [b] | 2.25 [b] | | |
| zni | $Zn(Im)_2$ | IMIDZB | 16 | 3611.7 [a] | 4.43 [a] | –3757.034 | –3757.822 |
| | | | | 3440.7 [b] | 4.66 [b] | | |

Table 1: Optimized geometry and experimentally determined parameters ([b]) of ZIFs (PhIm = benzimidazolate, mIm = methylimidazole); simulated with the $Zn(Im)_2$ composition. (*) and ([a]) refer to the model structures proposed by Lewis et al. [19]. The table shows the chemical composition, the

CCDC codes, the number of Zn atom per unit, the unit volume, the framework density (expressed as the number of Zn atoms per volume unit) and the total energies of different ZIF structures.

In Figure 1 we have plotted the calculated total energies of our ZIF structures as a function of their framework densities. The total energy of the most stable structure, zni, is taken as a reference point for the other energies.

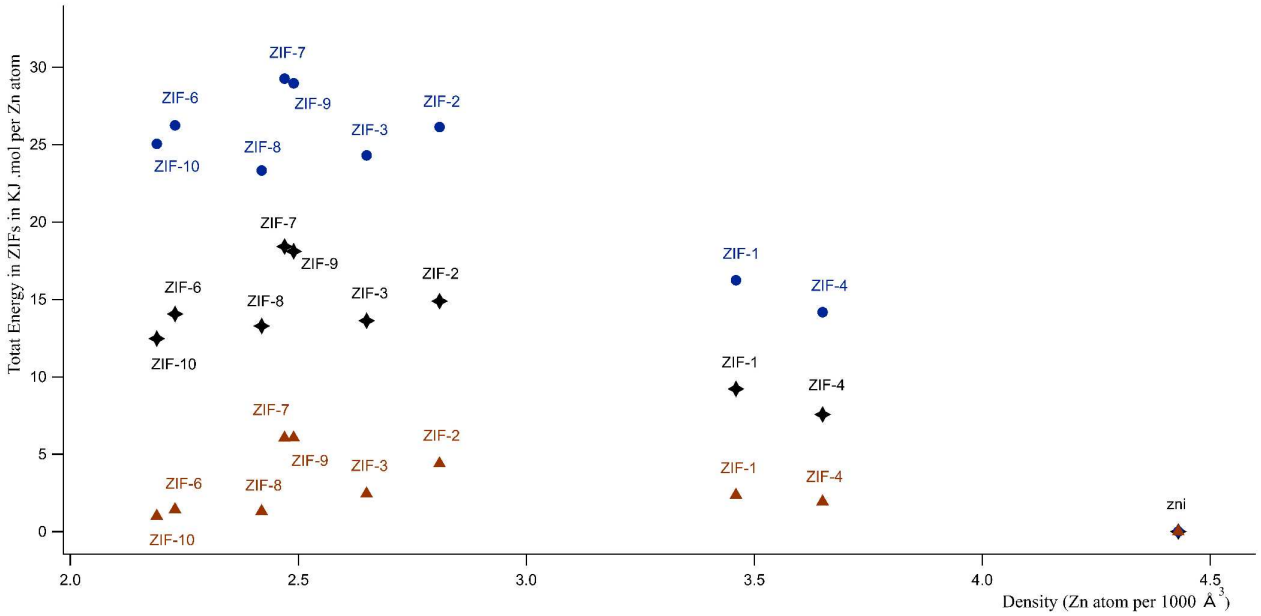


Figure 1: Variation of total energy of the ZIF using DFT method versus their framework density. zni energy taken as reference. (♦) Energy calculated by Lewis et al. [19]. The red triangles and the blue circles are our calculated PBE and PBE-D3 energy respectively.

It should be emphasized that the trend of the variation of our ZIFs energy calculated in terms of their framework densities is in excellent agreement with the one obtained by Lewis et al. [19]. We note that the synthesized ZIFs (ZIF-1 to ZIF-6, ZIF-10 and zni) present the most stable structures. For this set of materials, it is noticed that as the density increases, the ZIFs structures show generally more stability. The modified ZIF-7 and ZIF-9 are the less stable structures, probably due to the fact that there are no substituents in the imidazolate rings that can increase the number of possible hydrogen bonds and consolidate the ZIF. We observe that pure PBE systematically under-estimates the relative ZIF energy, compared to the results of Lewis et al. [19], but that conversely PBE-D3 tends to over-estimate the same relative energies. This highlights both the influence and subtle balance of dispersion interactions in ZIF structures.

## 2. Carbon dioxide adsorption

We have trapped one $CO_2$ molecule in the center of the cavity of each optimized ZIF structures obtained earlier in order to study their ability to adsorb one $CO_2$ molecule. The shape of the cavity and the pore size can differ from one ZIF to the other (i. e. the cavity of ZIF-8 contains 8 Zn atoms and 4 Zn atoms in ZIF-1). We will see later how this influences the interaction energy of $CO_2$ in the different ZIF structures.

We have performed a full geometry optimization with fixed cell parameters for each $CO_2$@ZIF complex. The complexes obtained are shown in Figure 2.

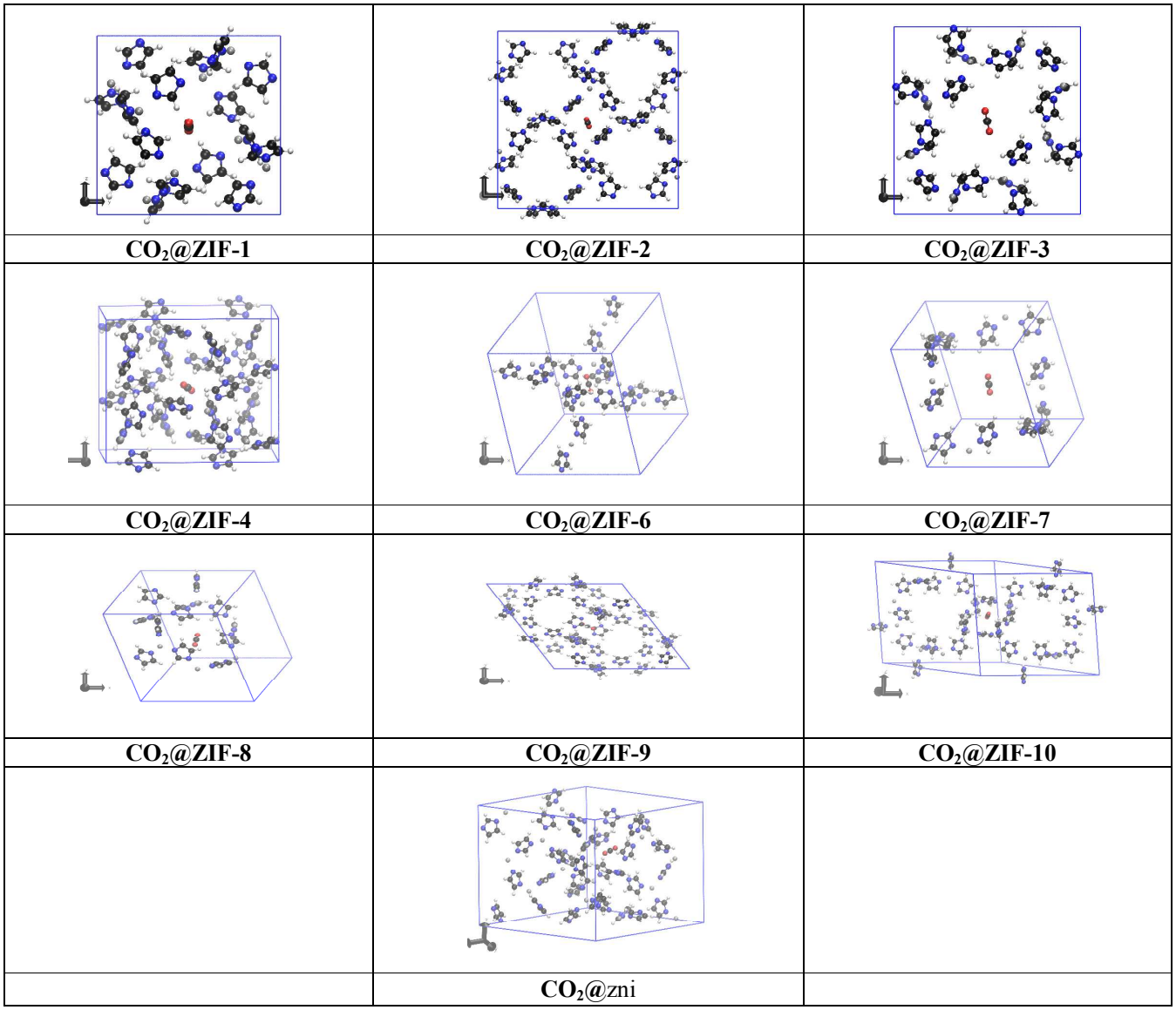


Figure 2: Optimized geometries of the different $CO_2$@ZIFs complexes where the $CO_2$ molecule is trapped in the cavity center of each ZIF structures.

We noticed that no geometrical distortion of the carbon dioxide molecule occurs, in the cavity center of the ZIF structures. The $CO_2$ molecule stays linear with equal CO bond lengths. The bond length of $CO_2$ is found to be 1.17 Å in all different sets of ZIF which it is in good agreement with the experimental value (1.16 Å) for the isolated molecule [27]. However, the trapped $CO_2$ molecule induces a structural distortion on most of the ZIF molecules; the imidazolate rings reorient itself towards the $CO_2$ molecule. Moreover, in

most of the $CO_2$@ZIF complexes, we observe a small variation of the Zn–Zn distances (0.01 Å) with respect to the starting values.

We also characterize the interactions between $CO_2$ and ZIF materials by means of the variation of the dipole moments before and after complexation (see Table 2). In most cases, ZIF-1, -2, -4, -6, -7, -9 and -10, the ZIF structures are initially apolar, the dipole moment calculated is nearly zero. ZIF-3 and -8 are weakly polar and the most stable structure, zni shows the largest dipole moment (1.73 Debye). After the complexation, the dipole moments vary slightly as reported in Table 2.

| ZIFs | Number of Zn atoms in ZIFs cavity | Dipole moments in Debye | |
|---|---|---|---|
| | | Clean structure | Complexed structure |
| 1 | 8 | 0.00 | 0.02 |
| 2 | 4 | 0.00 | 0.30 |
| 3 | 16 | 0.23 | 0.21 |
| 4 | 8 | 0.00 | 0.07 |
| 6 | 4 | 0.00 | 0.09 |
| 7* | 6 | 0.00 | 0.01 |
| 8* | 6 | 0.11 | 0.43 |
| 9* | 4 | 0.00 | 0.02 |
| 10 | 4 | 0.01 | 0.35 |
| Zni | 4 | 1.73 | 1.71 |

Table 2: Calculated dipole moments for the different ZIF structures before and after the complexation with the $CO_2$ molecule.

Using the DFT-D3/PBE method, we have calculated the interaction energy between the $CO_2$ molecule and the ZIF ($E_{int}(CO_2@ZIF)$) according to the following formula:

$$E_{int}(CO_2@ZIF) = E_{opt}(CO_2@ZIF) - [E_{opt}(ZIF) + E_{opt}(CO_2)]$$

where $E_{opt}(CO_2@ZIF)$, $E_{opt}(CO_2)$ and $E_{opt}(ZIF)$ are the total energies of the optimized geometries of the complex $CO_2$@ZIF, the isolated $CO_2$, and the isolated ZIF respectively. Our results are shown in Table 3, along with computed atomic charges and charge transfer estimation using Mulliken population analysis[28].

| ZIF | Net atomic charge (e) of $CO_2$ | | | Charge transfer (e) between CO2 and different ZIFs | $E_{int}$ ($CO_2$@ZIFs) in kJ $mol^{-1}$ |
|---|---|---|---|---|---|
| | C | O | O | | |
| 1 | **0.29011** | **–0.13910** | **–0.14468** | 0.00632 | –17.31 |
| | 0.30781 | –0.15393 | –0.15389 | | |
| 2 | **0.29556** | **–0.12740** | **–0.17541** | 0.00726 | –10.14 |
| | 0.31022 | –0.15511 | –0.15511 | | |
| 3 | **0.30343** | **–0.15161** | **–0.15292** | –0.00110 | –6.71 |
| | 0.31154 | –0.15572 | –0.15582 | | |
| 4 | **0.33953** | **–0.17462** | **–0.17070** | –0.00579 | –25.00 |
| | 0.31030 | –0.15515 | –0.15515 | | |
| 6 | **0.29375** | **–0.15030** | **–0.15535** | –0.01190 | 2.31 |
| | 0.31020 | –0.15510 | –0.15510 | | |
| 7 | **0.31138** | **–0.15438** | **–0.15683** | 0.00017 | –3.28 |
| | 0.31041 | –0.15517 | –0.15524 | | |
| 8 | **0.33529** | **–0.16983** | **–0.17137** | –0.00593 | –19.70 |
| | 0.31133 | –0.15566 | –0.15567 | | |
| 9 | **0.30744** | **–0.16094** | **–0.15521** | –0.00871 | –16.13 |
| | 0.31020 | –0.15509 | –0.15511 | | |
| 10 | **0.29409** | **–0.12418** | **–0.17825** | –0.00834 | –17.82 |
| | 0.31007 | –0.15502 | –0.15505 | | |
| zni | **0.29421** | **–0.14824** | **–0.13758** | 0.00839 | –27.71 |
| | 0.31011 | –0.15509 | –0.15502 | | |

Table 3: Calculated energies and charge transfer (Δρ) between $CO_2$ and the different ZIFs materials calculated as: $\Delta q = q(CO_2)_{ZIF} - q(CO_2)_{free}$ where $q(CO_2)_{ZIF}$ is the $CO_2$ charge molecule in ZIF material (in bold letters) and $q(CO_2)_{free}$ is the charge of $CO_2$ free molecule (normal letters).

All the results show a weak charge transfer between $CO_2$ and ZIFs indicating that we have a physisorption process. The data in the Table 3 shows that the interaction energy between $CO_2$ and the ZIFs in the cavity center is mainly dominated by Van der Waals forces. In general, we can conclude that as the ZIF cavity diameter decreases, the number of imidazolates linkers surrounding the $CO_2$ molecule increases and the interaction energy of $CO_2$@ZIFs increases. This is the case for $CO_2$ in a zni cavity. However, for ZIF-6 with a small central cavity, the $CO_2$@ZIF-6 complex has a positive value of the interaction energy. This shows the absence of a tendency to fix $CO_2$ despite a favorable charge transfer. For ZIF-3 and ZIF-7 the interaction energy is weak since these two materials have the largest cavity compared to the others ($d_{ZIF-3}$ = 8.02 Å, $d_{ZIF-7}$ = 4.31 Å; *d* is the diameter of the largest sphere that will fit into the framework [1]). Also, the insertion of $CO_2$ in these two cavities does not affect their geometries, this is confirmed by the low variation of their dipole moment (~0.01Debye).

To quantify the correlation between structural parameters and the interaction energy, we plotted the variation of the interaction energy of $CO_2$@ZIF complexes as a function of the ZIF framework densities expressed as the number of Zn sites per ZIF unit volumes (Figure 3).

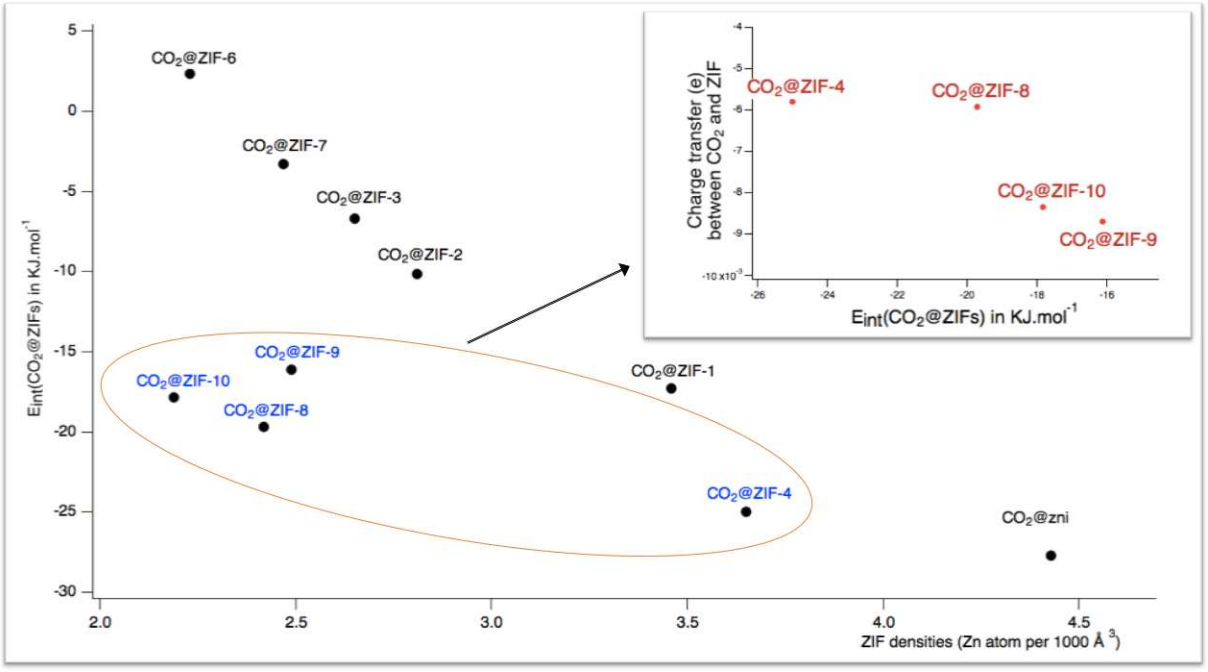


Figure 3: variation of $CO_2$@ZIF interaction energy as a function of ZIF framework densities expressed as the number of Zn sites per ZIF unit volumes. In the upper panel is and the charge transfer between $CO_2$ and ZIF as a function of $CO_2$@ZIF interaction energy.

It appears that two distinct groups can be identified among the known $CO_2$@ZIF complexes structures: a first group consisting of $CO_2$@ZIF-1, -2, -3, -6, -7, and zni where the $CO_2$@ZIF interaction energy and the ZIFs density framework varied concomitantly, and second group consisting of $CO_2$@ZIF-4, -8, -9, and -10, the most interacting complexes. For this last group, we looked to the variation of charge transfer between $CO_2$ and the ZIF structures as a function of interacting $CO_2$@ZIFs energy. We find that the charge transfers increase as the $CO_2$@ZIFs interaction energy increases.

Indeed, in ZIFs structures, the organic frameworks are linked to metal ions through nitrogen atoms which are the most active sites of the imidazolate ligands. In the presence of $CO_2$, the attachment occurs through NNCH—OCO or CH–CH—OCO hydrogen-like bonds or through π-staking interactions depending on the orientation of the imidazolate linkers in the ZIF cavity. More details are provided in the next section.

## 3. The charge transfer analysis

The process of $CO_2$ adsorption by zeolitical imidazolate frameworks occurs through a physisorption interaction. In order to understand the nature of the binding process, we have calculated the charge density difference Δρ for the different $CO_2$@ZIF complexes using the following formula:

$$\Delta\rho = \rho(CO_2@ZIFs) - \rho(CO_2) - \rho(ZIF)$$

where $\rho(CO_2@ZIFs)$ is the charge density of the $CO_2$@ZIF complex; $\rho(CO_2)$ and $\rho(ZIF)$ are the charge densities of the non-interacting $CO_2$ and ZIF molecules respectively at the geometry of the complex.

Our computed charge densities differences are plotted in Figure 3 to allow for a better understanding of the $CO_2$@ZIF interactions and explain the variations of the interaction energies calculated for the different $CO_2$@ZIF complexes. Two interaction cases occur: low charge density transfer for $CO_2$@ZIF-3 and $CO_2$@ZIF-7 and strong interaction for the rest of the $CO_2$@ZIFs complexes.

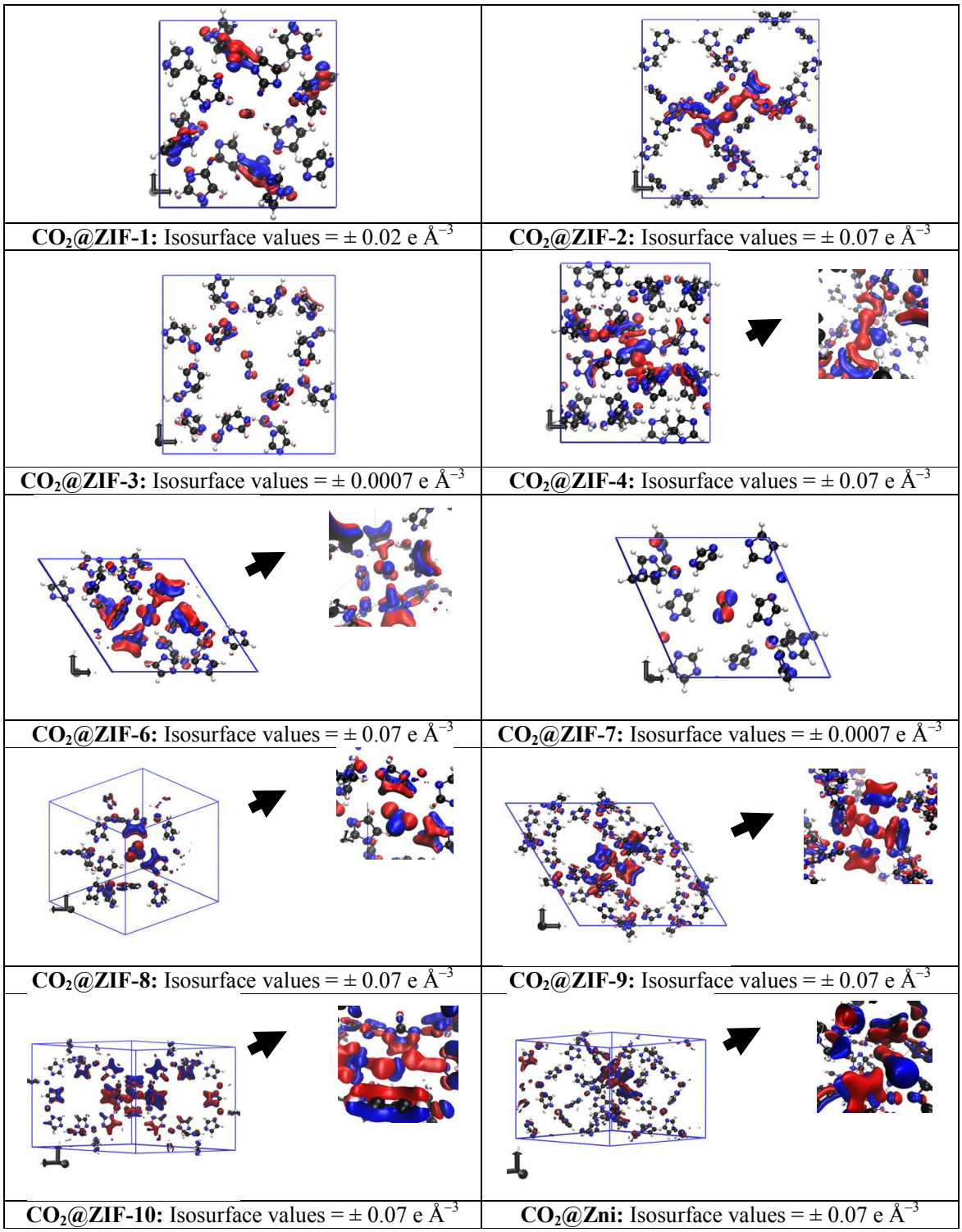


Figure 4: Charge density calculated for different $CO_2$@ZIF complexes. Regions of accumulation/depletion are marked in blue/red, respectively.

In figure 4 we used different iso-charge surfaces to better display the computed charge density transfer. The classification of the interaction energies is shown in Table 3. Interestingly, the charge density

transfer between $CO_2$ and ZIF-9 shows that $CO_2$ is fixed trough π-staking interactions with the two close imidazolates. For $CO_2$@ZIF-10 the interaction originates from the formation of two hydrogen bonds.

## 4. Conclusion

In the present work, we carried out a comparative study of the adsorption of a $CO_2$ molecule by different zeolitic imidazolate framework materials. This study examines two types of structures: the synthesized one (ZIF-1 to -4, -6, -10 [1] and zni [18]) and the proposed models by Lewis (ZIF-7 to -9 [19]). The common point is that they have all the same chemical composition $Zn(Im)_2$. Using DFT/PBE and DFT-D3/PBE calculations, we have shown that the capture of the carbon dioxide depends on the nature of the dimension of the cavity in which it is inserted; as it increases, the interaction energy of $CO_2$@ZIF decreases. We have also validated the two proposed ZIF structures ZIF-8 and ZIF-9 for $CO_2$ capture.

The capture of $CO_2$ is due to physisorption phenomena. To understand the nature of the interactions of $CO_2$ in the ZIFs cavity, we have calculated the charge density which recalls the formation of two type of $CO_2$ attachment: π-stacking and hydrogen-like bond.

We have shown that the insertion of a $CO_2$ molecule in the different ZIF cavities induces a rearrangement of the imidazolate linkers and a slight variation of the dipole moments for the different ZIF structures is observed. The capture of $CO_2$ occurs without any structural distortion for the guest molecule. This allows us to start thinking about how to make this molecule more active.

The simple model proposed in this work using single $CO_2$ molecule in the center of the ZIF cavities to describe $CO_2$ capture by zeolitic imidazolate frameworks may not be sufficient to describe all $CO_2$–ZIF interactions. In addition, the presence of several $CO_2$ molecules requires to also consider the $CO_2$–$CO_2$ interactions[29], this could be the subject of a future work in this field.

## Acknowledgements

This work has been carried out in the context of the European PF7 Marie Curie IRSES-GA-2012-317544 Project CapZeO. We thank the Moroccan Association of Theoretical Chemists (A.M.C.T), the C.N.R.S.T. (National Center for Research and Technology) for their support and the usage of computer facilities at the University of Hull.

## References

(1) Park, K. S.; Ni, Z.; Côté, A. P.; Choi, J. Y.; Huang, R.; Uribe-Romo, F. J.; Chae, H. K.; O'Keeffe, M.; Yaghi, O. M. Exceptional Chemical and Thermal Stability of Zeolitic Imidazolate Frameworks. *Proc. Natl. Acad. Sci.* **2006**, *103* (27), 10186–10191.

(2) Li, Y.; Yu, J. New Stories of Zeolite Structures: Their Descriptions, Determinations, Predictions, and Evaluations. *Chem. Rev.* **2014**, *114* (14), 7268–7316.

(3) Chen, B.; Yang, Z.; Zhu, Y.; Xia, Y. Zeolitic Imidazolate Framework Materials: Recent Progress in Synthesis and Applications. *J. Mater. Chem. A* **2014**, *2* (40), 16811–16831.

(4) Wang, B.; Côté, A. P.; Furukawa, H.; O'Keeffe, M.; Yaghi, O. M. Colossal Cages in Zeolitic Imidazolate Frameworks as Selective Carbon Dioxide Reservoirs. *Nature* **2008**, *453* (7192), 207–211.
(5) Banerjee, R.; Furukawa, H.; Britt, D.; Knobler, C.; O'Keeffe, M.; Yaghi, O. M. Control of Pore Size and Functionality in Isoreticular Zeolitic Imidazolate Frameworks and Their Carbon Dioxide Selective Capture Properties. *J. Am. Chem. Soc.* **2009**, *131* (11), 3875–3877.
(6) McDaniel, J. G.; Yu, K.; Schmidt, J. R. Ab Initio, Physically Motivated Force Fields for CO2 Adsorption in Zeolitic Imidazolate Frameworks. *J. Phys. Chem. C* **2012**, *116* (2), 1892–1903.
(7) Liu, J.; Keskin, S.; Sholl, D. S.; Johnson, J. K. Molecular Simulations and Theoretical Predictions for Adsorption and Diffusion of CH4/H2 and CO2/CH4 Mixtures in ZIFs. *J. Phys. Chem. C* **2011**, *115* (25), 12560–12566.
(8) Liu, Y.; Liu, J.; Chang, M.; Zheng, C. Effect of Functionalized Linker on CO2 Binding in Zeolitic Imidazolate Frameworks: Density Functional Theory Study. *J. Phys. Chem. C* **2012**, *116* (32), 16985–16991.
(9) Han, S. S.; Kim, D.; Jung, D. H.; Cho, S.; Choi, S.-H.; Jung, Y. Accurate Ab Initio-Based Force Field for Predictive CO2 Uptake Simulations in MOFs and ZIFs: Development and Applications for MTV-MOFs. *J. Phys. Chem. C* **2012**, *116* (38), 20254–20261.
(10) Salah, M.; Marakchi, K.; Dalbouha, S.; Senent, M. L.; Kabbaj, O. K.; Komiha, N. Influence of the Functionalization of Imidazole on Its CO2 Uptake Efficiency. A Theoretical Contribution. *Comput. Theor. Chem.* **2015**, *1073*, 1–8.
(11) Boulmene, R.; Boussouf, K.; Prakash, M.; Komiha, N.; Al-Mogren, M. M.; Hochlaf, M. Ab Initio and DFT Studies on CO2 Interacting with Znq+–Imidazole (Q=0, 1, 2) Complexes: Prediction of Charge Transfer through σ- or π-Type Models. *ChemPhysChem* **2016**, *17* (7), 994–1005.
(12) VandeVondele, J.; Krack, M.; Mohamed, F.; Parrinello, M.; Chassaing, T.; Hutter, J. Quickstep: Fast and Accurate Density Functional Calculations Using a Mixed Gaussian and Plane Waves Approach. *Comput. Phys. Commun.* **2005**, *167* (2), 103–128.
(13) CP2K developers group, CP2K Code.http://www.cp2k.org .
(14) Hohenberg, P.; Kohn, W. Inhomogeneous Electron Gas. *Phys. Rev.* **1964**, *136* (3B), B864–B871.
(15) Kohn, W.; Sham, L. J. Self-Consistent Equations Including Exchange and Correlation Effects. *Phys. Rev.* **1965**, *140* (4A), A1133–A1138.
(16) Lippert, B. G., Hutter, J., and Parrinrllo, M. A hybrid Gaussian and plane wave density functional scheme. Mol. Phys. 1997, 92, 477–488.
(17) Perdew, J. P.; Chevary, J. A.; Vosko, S. H.; Jackson, K. A.; Pederson, M. R.; Singh, D. J.; Fiolhais, C. Atoms, Molecules, Solids, and Surfaces: Applications of the Generalized Gradient Approximation for Exchange and Correlation. *Phys. Rev. B* **1992**, *46* (11), 6671–6687.
(18) Lehnert, R.; Seel, F. Darstellung Und Kristallstruktur Des Mangan(II)- Und Zink(II)-Derivates Des Imidazols. *Z. Für Anorg. Allg. Chem.* **1980**, *464* (1), 187–194.
(19) Lewis, D. W.; Ruiz-Salvador, A. R.; Gómez, A.; Rodriguez-Albelo, L. M.; Coudert, F.-X.; Slater, B.; Cheetham, A. K.; Mellot-Draznieks, C. Zeolitic Imidazole Frameworks: Structural and Energetics Trends Compared with Their Zeolite Analogues. *CrystEngComm* **2009**, *11* (11), 2272–2276.
(20) The Cambridge Crystallographic Data Centre, CCDC. www.ccdc.cam.ac.uk
(21) Grimme, S., Antony, J., Ehrlich, S., & Krieg, H. A consistent and accurate ab initio parametrization of density functional dispersion correction (DFT-D) for the 94 elements H-Pu. J. Chem. Phys. 2010, 132, 154104.
(22) VandeVondele, J., & Hutter, J. Gaussian basis sets for accurate calculations on molecular systems in gas and condensed phases. J. Chem. Phys. 2007,127, 114105.
(23) Hartwigsen, C.; Goedecker, S.; Hutter, J. Relativistic Separable Dual-Space Gaussian Pseudopotentials from H to Rn. *Phys. Rev. B* **1998**, *58* (7), 3641–3662.
(24) Goedecker, S.; Teter, M.; Hutter, J. Separable Dual-Space Gaussian Pseudopotentials. *Phys. Rev. B* **1996**, *54* (3), 1703–1710.
(25) Krack, M. Pseudopotentials for H to Kr Optimized for Gradient-Corrected Exchange-Correlation Functionals. *Theor. Chem. Acc.* **2005**, *114* (1–3), 145–152.
(23) VandeVondele, J., & Hutter, J. An efficient orbital transformation method for electronic structure calculations. J. Chem. Phys. 2003 ,118, 4365–4369.

(27) Khot, K. M.; Heer, P. K. K. S.; Biniwale, R. B.; Gaikar, V. G. Equilibrium Adsorption Studies of CO2, CH4, and N2 on Amine Functionalized Polystyrene. *Sep. Sci. Technol.* **2014**, *49* (15), 2376–2388.

(28) Mulliken, R. S. Electronic Population Analysis on LCAO–MO Molecular Wave Functions. I. *J. Chem. Phys.* **1955**, *23* (10), 1833–1840.

(29) Moghadam, P. Z.; Ivy, J. F.; Arvapally, R. K.; Santos, A. M. dos; Pearson, J. C.; Zhang, L.; Tylianakis, E.; Ghosh, P.; Oswald, I. W. H.; Kaipa, U.; et al. Adsorption and Molecular Siting of CO2, Water, and Other Gases in the Superhydrophobic, Flexible Pores of FMOF-1 from Experiment and Simulation. *Chem. Sci.* **2017**, *8* (5), 3989–4000.

# TOC graphic

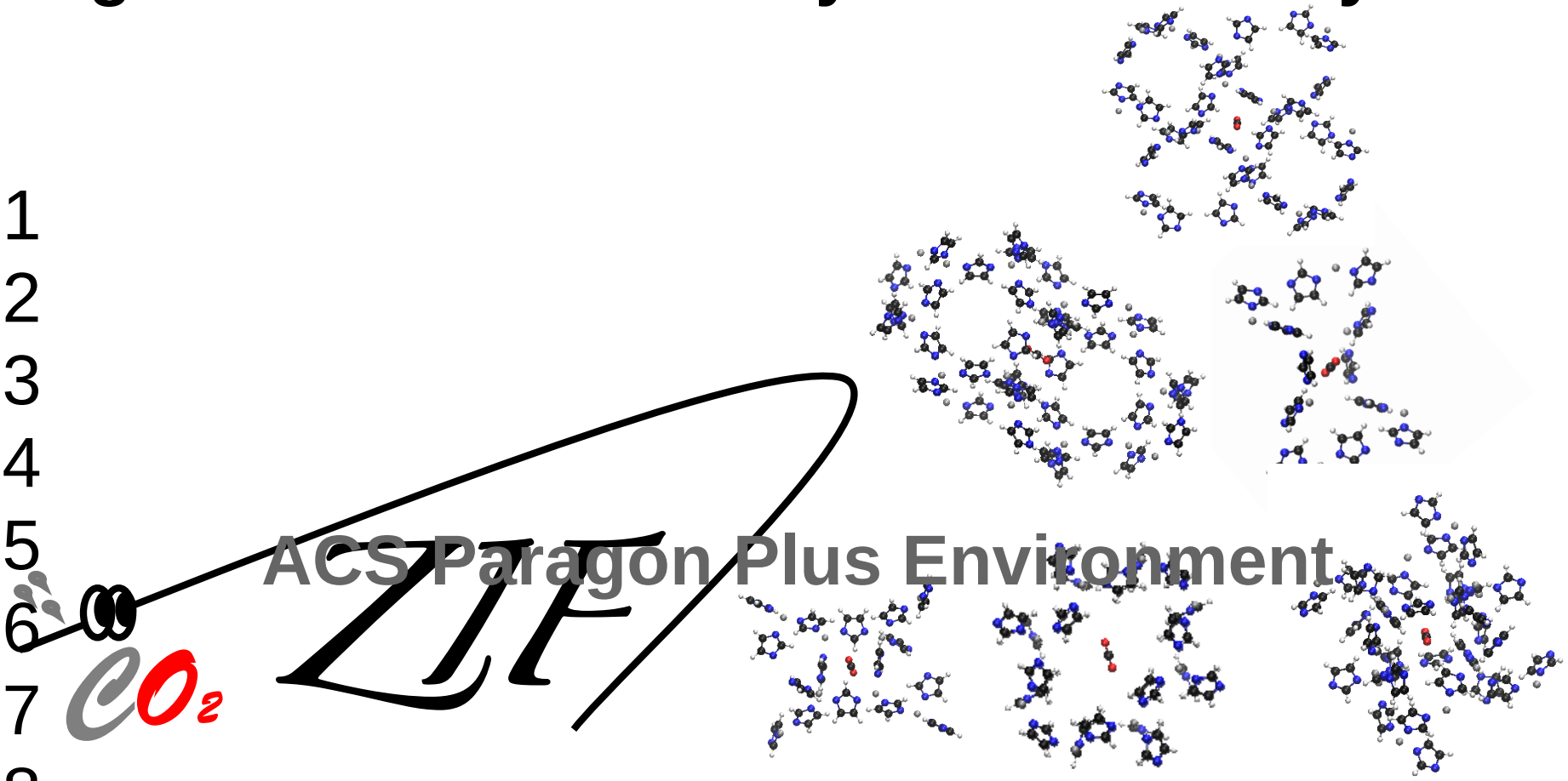
ZIF
CO2
ACS Paragon Plus Environment